Noncovalent PEGylation via Lectin–Glycopolymer Interactions

Journal:	*Biomacromolecules*
Manuscript ID	bm-2016-00766s.R1
Manuscript Type:	Article
Date Submitted by the Author:	n/a
Complete List of Authors:	Antonik, Pawel; National University of Ireland, Galway Eissa, Ahmed; University of Warwick, Round, Adam; ESRF Cameron, Neil; Monash University, Dept of Materials Science and Engineering Crowley, Peter; National University of Ireland, Galway,

Noncovalent PEGylation *via* Lectin–Glycopolymer Interactions

Paweł M. Antonik,[a,b] Ahmed M. Eissa,[c,d,e] Adam R. Round,[f] Neil R. Cameron,[c,d] and Peter B. Crowley[a,]*

[a]School of Chemistry, National University of Ireland Galway, University Road, Galway, Ireland.

[b]Teagasc Food Research Centre, Ashtown, Dublin 15, Ireland.

[c]Department of Chemistry, Durham University, Science Laboratories, South Road, Durham DH1 3LE, United Kingdom.

[d]Present addresses: School of Engineering, University of Warwick, Coventry, CV4 7AL, United Kingdom; Department of Materials Science and Engineering, Monash University, Clayton 3800, Victoria, Australia.

[e]Department of Polymers, Chemical Industries Research Division, National Research Centre (NRC), El-Bohoos Street, Dokki, Cairo, Egypt.

[f]European Molecular Biology Laboratory Grenoble Outstation, 71 Avenue des Martyrs, 38042 Grenoble Cedex 9, France and Faculty of Natural Sciences, Keele University, Keele, Staffordshire, ST5 5BG, UK.

*Correspondence to: peter.crowley@nuigalway.ie, +353 91 49 24 80

Keywords:
PEGylation, protein-polymer conjugate, radius of gyration, NMR spectroscopy, SAXS

Abstract

PEGylation, the covalent modification of proteins with polyethylene glycol, is an abundantly used technique to improve the pharmacokinetics of therapeutic proteins. The drawback with this methodology is that the covalently attached PEG can impede the biological activity (*e.g.* reduced receptor-binding capacity). Protein therapeutics with "disposable" PEG modifiers have potential advantages over the current technology. Here, we show that a protein-polymer "Medusa complex" is formed by the combination of a hexavalent lectin with a glycopolymer. Using NMR spectroscopy, small angle X-ray scattering (SAXS), size exclusion chromatography and native gel electrophoresis it was demonstrated that the fucose-binding lectin RSL and a fucose-capped polyethylene glycol (Fuc-PEG) form a multimeric assembly. All of the experimental methods provided evidence of noncovalent PEGylation with a concomitant increase in molecular mass and hydrodynamic radius. The affinity of the protein-polymer complex was determined by ITC and competition experiments to be in the μM range, suggesting that such systems have potential biomedical applications.

Introduction

The modification of proteins with synthetic polymers is a powerful route to novel functionalized macromolecules with applications in biotechnology and medicine.[1–7] PEGylation, the covalent attachment of polyethylene glycol, is a versatile means to increase a protein's size, stability and solubility.[2,8–11] The increased radius of protein-PEG conjugates leads to a reduction in renal filtration, which together with decreased immunogenicity can result in longer circulation half lives compared to the native protein.[9,10] Such improvements in pharmacokinetics are crucial for the development of cost-effective and patient-friendly protein therapeutics. However, PEGylation can also interfere with the processes of molecular recognition and lead to reduced biological activity. Steric hindrance of the binding site by PEG can impede complex formation with the target receptor.[9,10] This effect may be eliminated in poly(zwitterion)-based conjugates.[4] Furthermore, reversible PEGylation strategies have been developed that take advantage of slowly hydrolysable,[12,13] light-sensitive[14] or thiol-sensitive[15] linkers to release the PEG component.

With the growing demand for tunable protein-polymer macromolecules the focus of attention is shifting towards noncovalent conjugates.[16–26] Examples include polymer conjugation *via*: co-factor reconstitution,[16] the biotin-streptavidin complex,[18] supramolecular complexation with cucurbituril,[19] charge-charge[20] and metal affinity[21,24] interactions, as well as lectin-mediated complexation.[25,27,28] The advantage of noncovalent systems is that temporal control of conjugate assembly and disassembly can be asserted by the presence of competitor molecules.[19] In the context of protein therapeutics it is envisaged that the biologically-active ligand-receptor complex may act as a competitor to displace the lower affinity polymer interaction. Thus, the potential interference caused by covalently attached PEG chains will be minimised. Noncovalent PEGylation involves several challenges, the foremost being the control of the protein-polymer affinity which must be sufficiently high to enable the positive effects of PEGylation (*i.e.* increased circulation half life) and yet low enough to permit transient unbinding and competition by the host receptor (K_d ~nM-μM). Coupled to this challenge is the need for simple linker chemistries which are biocompatible, synthetically attractive and inexpensive.

At this point we note that the study of noncovalent protein-PEG assemblies is not new. Early applications were focused on protein purification by phase separation in mixtures of dextran and dye-conjugated PEG.[29–31] Figure 4 in reference 30 is startling in its originality and relevance to current developments.

Here, we have combined a fucose-binding lectin with a fucose-capped polyethylene glycol (Fuc-PEG) to produce a noncovalent protein-polymer "Medusa complex" (Figure 1). RSL, a hexavalent fucose-binding lectin from *Ralstonia solanacearum*, was chosen as the model protein for this study. RSL is a well-characterized ~29 kDa trimer with three intra-monomeric and three inter-monomeric binding sites for L-fucose and related sugars.[32–35] Building on current developments in the structural characterization of PEGylated proteins,[11,36] we have used TROSY NMR spectroscopy to demonstrate protein-polymer noncovalent conjugation via the fucose-binding site. The formation of high molecular weight protein-polymer particles was confirmed by size exclusion chromatography (SEC), small angle X-ray scattering (SAXS) and electrophoresis experiments. SAXS analysis further revealed a core structure bearing six PEG tails with random coil conformations. Competition binding experiments demonstrated that the Fuc-PEG appendages could be displaced by methyl-α-L-fucoside (Me-fuc) but not by L-galactose (L-gal). Together, these data indicate that reversible protein-polymer conjugates were formed from the combination of a carbohydrate binding protein and a sugar-functionalized polymer. This strategy of noncovalent PEGylation may benefit the development of lectin-mediated drug delivery systems.[37–39]

Materials and Methods

Materials. Methyl-α-L-fucoside (Me-fuc) and L-galactose (L-gal) were purchased from Carbosynth and Sigma, respectively. L-fucose-capped polyethylene glycol (Fuc-PEG) was synthesized via a copper catalyzed azide-alkyne cycloaddition[40] (Supporting Information, Scheme S1). Alkyne terminated PEG (Alk-PEG) was prepared according to an adapted literature procedure,[41] by using PEG monomethyl ether (~2 kDa, Sigma 202509) and propargyl bromide. The ^{1}H NMR spectrum of Alk-PEG included peaks at 2.42 and 4.18 ppm, assigned to the alkyne proton and the adjacent CH_2 protons, respectively (Figure S1). 2-azidoethyl α-L-fucose was synthesized as described.[42] For the click reaction, stoichiometric amounts of Alk-PEG and 2-azidoethyl α-L-fucose were combined in t-butanol/water (5:1) in the presence of copper sulfate (0.1 eq.) and sodium ascorbate (0.2 eq.) at 50 °C for 24 h (Figures S1 and S2). The product was purified by flash chromatography and formation of the triazole was confirmed by ^{1}H NMR (Figure S2) and ATR-FTIR spectroscopy (Figure S3).

Protein samples. RSL was produced in *E. coli* BL21, transformed with the plasmid pET25rsl, and purified by mannose-affinity chromatography.[32] The ^{15}N-labeled protein was prepared as described recently.[35]

Size exclusion chromatography. SEC was carried out at 21° C on an Äkta FPLC equipped with an XK 16/70 column (1.6 cm diameter, 65 cm bed-height) packed with Superdex 75 (GE Healthcare). Filtered, degassed buffer (20 mM KPi, 50 mM NaCl, pH 6.0) was used at a constant flow rate of 1.5 mL/min. The samples (800 µL) contained RSL (0.25 mM) with 12 eq. of Fuc-PEG or Me-fuc. Sample elution was monitored at 280 nm.

Electrophoretic characterization of noncovalent PEGylation. Native electrophoresis was performed using 5% polyacrylamide or 2% agarose gels (6.0 cm x 7.0 cm) in horizontal mode. The samples (15 µL) contained 100 µM RSL and up to 12 equivalents of Fuc-PEG. Acrylamide gels were run at a constant voltage of 150 V in Tris/Gly buffer at pH 8.3 for 30 min. Agarose gels were run at 100 V in 20 mM KPi at pH 6.0 for 20 min. Visualization of the protein migration was achieved with Coomassie staining and a flatbed scanner.

NMR characterization. ^{1}H-^{15}N TROSY-HSQC[43,44] spectra were acquired at 303 K on an Agilent 600 MHz NMR spectrometer equipped with a HCN cold probe. The samples contained 0.25 or 0.5 mM ^{15}N-RSL in the sugar-free form or in the presence of 1-12 equivalents of Fuc-PEG, methyl-α-L-fucoside or L-galactose. The buffer (20 mM potassium phosphate, 50 mM NaCl, pH 6.0) was identical for all samples. The data were processed in NMRPipe.[45] Differences in chemical shifts (Δδ) between the sugar-free and -bound forms of RSL were measured in CCPN[46] and the average perturbations were calculated as $\Delta\delta_{avg} = \{[\Delta\delta_H^2 + (0.2 \times \Delta\delta_N^2)]/2\}^{½}$.[35,47]

Isothermal titration calorimetry. Experiments were performed at 25° C using a Nano ITC (TA Instruments) and conditions similar to those previously published.[32] Samples of protein (24 μM) and ligands (1-2 mM) were prepared in identical buffer (0.1 M Tris-HCl, pH 7.5). Ligand solutions were added in 30 injections of 3 μl at intervals of 3 min while stirring at 300 rpm. A control experiment was performed by injecting Fuc-PEG into buffer, which yielded negligible heats of dilution. The data analysis was performed in NanoAnalyze.

SAXS characterization. Small-angle X-ray scattering experiments were performed at the ESRF BioSAXS beamline BM29 equipped with a Pilatus 1M detector (Dectris).[48,49] RSL bound to Me-fuc or to Fuc-PEG was characterized at four different protein concentrations (10, 5, 2 and 1 mg/ml) using the automated sample changer.[50] Data were collected also on a sample of the conjugate that was pre-treated via an online SEC at BM29.[51] All of the samples were prepared in the same buffer, identical to that used for the NMR experiments. 55 (automated sample changer) or 100 (SEC) μl volumes were exposed to X-rays for 10 individual frames, each 1 second in duration. Individual frames were processed with the automatic processing pipeline[52], to yield individual radially-averaged curves of normalized intensity versus scattering angle $s = 4\pi\sin\theta/\lambda$. Additional data reduction in EDNA utilized the automatic data processing tools of the EMBL-Hamburg ATSAS package[53,54] to combine timeframes (excluding any data points affected by radiation damage), yielding the average scattering curve for each exposure series. Matched buffer measurements taken before and after every sample were averaged and used for background subtraction. Merging of separate concentrations and further analysis were performed manually using the ATSAS package.[55]

The forward scattering $I(0)$ and radius of gyration R_g were calculated from the Guinier approximation.[56] The hydrated particle volume was computed using the Porod invariant[57] and the maximum particle size D_{max} was determined from the pair distribution function computed by GNOM[58] in PRIMUS.[59] An estimate of the molecular mass (MM) of each construct was made from the I(0), with the partial specific volumes of RSL and PEG taken as 0.74 and 0.83 cm^3/g, respectively.[60] *Ab initio* models were calculated using DAMMIF[61] and then averaged, aligned and compared in DAMAVER.[62] CRYSOL[63] was used to calculate the scattering of RSL based on the crystal structure coordinates[32] (PDB 2BT9). In CORAL, 6 x 22 dummy residues with random coil conformations (P_1 symmetry) were added to account for the six Fuc-PEG chains. The assumption of 22 residues per Fuc-PEG was based on the molecular weight (~2.3 kDa) and Svergun's demonstration that the electron density of PEG (~0.4 e/Å^3) is comparable to that of protein.[60] The averaged and filtered model was used to visualize the protein-polymer assembly and SUPCOMB[64] was used to optimally orient the RSL crystal structure (with minimal spatial discrepancy) into the final model. Fits of the models to the experimental data were prepared in SAXSVIEW (http://saxsview.sourceforge.net).

Results and Discussion

Biochemical characterization of RSL bound to Fuc-PEG. The formation of a noncovalent conjugate between RSL and Fuc-PEG was expected to yield a particle of ~50 % increased mass (compared to RSL, ~29 kDa). Assuming that all six sugar-binding sites are occupied by Fuc-PEG (~2.3 kDa) the conjugate will have a mass of ~43 kDa.

An initial characterization of the conjugate was performed by using size exclusion chromatography. RSL in the presence of 12 equivalents of Me-fuc (K_d ~0.6 μM[32]) eluted at ~75 mL (Figure S4). This elution volume was higher than expected (the ~31 kDa DNase eluted at ~65 mL) and suggests that RSL interacted weakly with the Superdex resin. In the presence of Fuc-PEG, elution was observed at ~55 mL, which corresponds to proteins of ~66 kDa (as indicated by a BSA standard). This higher-than-expected mass is characteristic of PEGylated proteins as the random coil nature of PEG occupies a larger volume than a corresponding mass of folded protein.[11,65,66] The peak at ~43 mL, corresponding to the void volume, suggested the presence of high molecular weight aggregates.[67]

The conjugate was further characterized by native gel electrophoresis. Samples of sugar-free RSL or RSL in the presence of Fuc-PEG were analysed in polyacrylamide or agarose gels (Figure 2). Consistent with the theoretical p*I* of ~6.5, RSL and the conjugate migrated towards the anode or cathode at pH 8.3 or pH 6.0, respectively. In the sugar-free form a diffuse protein band was observed. With increasing amounts of Fuc-PEG the migration distance was decreased. This observation suggests that noncovalent PEGylation produced larger particles that were more effectively retarded by the gel.

NMR characterization. ^{15}N-labelled RSL was titrated with μL aliquots of Fuc-PEG (10 mM stock) and monitored by ^{1}H-^{15}N TROSY-HSQC spectroscopy. The TROSY was necessary to improve spectral quality, consistent with the increased molecular mass and longer tumbling time of the conjugate (Figure S5 shows a comparison of the HSQC and TROSY-HSQC spectra of RSL bound to Fuc-PEG). The protein-polymer interaction was in slow-exchange on the NMR timescale consistent with an equilibrium dissociation constant in the micromolar range.[35,47] Considering the overall similarity of the spectra of RSL bound to Me-fuc and RSL bound to Fuc-PEG (Figure S6) it was evident that the highly-stable RSL structure[32] was unaltered by interaction with the polymer.

Figure 3 shows spectral regions of the superposed ^{1}H-^{15}N TROSY-HSQC of sugar-free RSL and RSL in the presence of Fuc-PEG or Me-fuc. Recently, we assigned the backbone resonances of RSL in the sugar-free form and in the presence of fucose-like sugars including Me-fuc.[35] Numerous resonances assigned to backbone and tryptophan indole nuclei in the sugar-binding sites had similar chemical shift perturbations ($\Delta\delta$) in the presence of Fuc-PEG or Me-fuc (Figure 3C). The similar pattern of shifts for each ligand indicated that Fuc-PEG binds to RSL in a fashion similar to Me-fuc. Interestingly, only two backbone resonances showed substantially different $\Delta\delta$ due to Fuc-PEG binding. The $\Delta\delta_{avg}$ for Lys34 and Asn79 in the presence of Fuc-PEG were >2 times larger than in the Me-fuc form (Figure 3C). Lys34 and Asn79 are structurally equivalent residues located in loops that flank the inter- and intra-monomeric sugar binding sites, respectively.[32,35] The backbone N atom of these residues is within 7.8 Å of the methyl substituent of Me-fuc in the RSL crystal structure (PDB 2BT9).[32] The large $\Delta\delta$ observed for these resonances (relative to the Me-fuc data) is evidence that the bulky Fuc-PEG polymer interacts at these sites. Note that the adjacent residues (33, 35 and 78, 80) are glycines and no amide resonances were observed in the sugar-free[35] or in the polymer-bound form.

The ~50 % increase in molecular mass of the RSL conjugate was expected to result in increased line widths of the NMR signals. In the presence of Me-fuc the average $^{1}H^{N}$ resonance line width of RSL was 19.8 (±2.3) Hz. In the presence of 12 equivalents Fuc-PEG the majority of the resonances demonstrated increased line widths and the average was 28.6 (±4.1) Hz (Table S1). This line broadening indicates an increased rotational correlation time consistent with the higher molecular weight of the complex with Fuc-PEG. The average broadening increase of ~8 Hz due to six PEG chains (each ~2 kDa) contrasts with the ~1 Hz broadening observed for a monoPEGylated protein with 5 kDa PEG.[11] Considering the possible contribution of aggregation (Figure S4) to the NMR data, a sample of RSL and 12 equivalents of Fuc-PEG was analysed by TROSY NMR before and after purification by SEC. The pre- and post-SEC samples yielded similar NMR spectra and the average line width was 26.0 (±4.4) Hz for the purified complex. Therefore, it can be concluded that the observed line width changes were due to noncovalent PEGylation (rather than aggregation).

To assess whether the PEG alone contributed to the observed chemical shift perturbations control experiments were performed using PEG 2000 (the starting material for the Fuc-PEG synthesis). There were no appreciable effects on the NMR spectrum of RSL (Figure S7)

indicating that PEG 2000 did not bind at this concentration (3 mM).[68] This result confirmed that the L-fucose cap was necessary for interaction.

Competition binding experiments were used to assess the binding affinity of RSL for Fuc-PEG. The pre-formed complex of 0.25 mM RSL in presence of 6 equivalents (1.5 mM) of Fuc-PEG was treated with 1.5 mM of Me-fuc or L-gal. Examination of the tryptophan indole resonances (Figure 4), which are excellent reporters of sugar binding,[35] indicated that the Fuc-PEG appendages were displaced by Me-fuc (K_d ~ 0.6 μM[32]) but not by L-gal (K_d ~ 9.0 μM[32]). The indole resonances of RSL bound to Fuc-PEG were shifted upon the addition of Me-fuc (compare Figure 3B). Interestingly, the structurally equivalent W31 and W76 had split resonances (Figure 4, blue contours) suggesting that the Fuc-PEG was not completely displaced. In contrast the spectrum of RSL bound to Fuc-PEG was completely unchanged by the addition of the weaker binding L-gal. These experiments proved the noncovalent / reversible nature of the interaction between RSL and Fuc-PEG. ITC was used to further characterize the complex of RSL with Fuc-PEG (Figure S8). The fit parameters matched previously published data for Me-fuc,[32,34] and the measured K_d (1.3 ±0.3 μM) was consistent with the results of the competition experiments.

Small angle X-ray scattering. RSL samples, at a maximum concentration of ~10 mg/mL, bound to Me-fuc or Fuc-PEG were characterised by SAXS. Data collection was performed using both the automated sample changer and the online SEC at BM29. The online SEC was used to remove high molecular weight aggregates (>150 kDa, Figure S4) immediately prior to data collection. The molecular mass (MM), the radius of gyration (R_g), the maximum particle size (D_{max}), and the volume (V) of RSL bound to Me-fuc were estimated at 27 ±3 kDa, 1.8 ±0.1 nm, 4.8 ±0.2 nm, and 42 nm^3, respectively. These parameters coincide, within error, with those computed from the RSL crystal structure (PDB 2BT9). The predicted scattering curve (CRYSOL) from the crystal structure fits neatly to the experimental data (χ = 1.97, Figure 5). *Ab initio* models calculated in DAMMIF[61] (with P_1 or P_6 symmetry, Figure 5) matched the crystal structure (Figure 6). All of these data confirmed that RSL is a trimer in solution.

Samples of RSL bound to Fuc-PEG resulted in a significant change to the scattering pattern (Figure 5). The parameters MM, R_g, D_{max}, and V increased to 42 ±5 kDa, 2.9 ±0.1 nm, 10.0 ±0.2 nm, and 72 nm^3, respectively, consistent with the formation of the protein-polymer

conjugate. The difference in molecular weight between RSL bound to Me-fuc and RSL bound to Fuc-PEG was ~15 kDa in agreement with the expected mass difference of 13.8 kDa. *Ab initio* models generated in DAMMIF[61] had six, three or one elongated protrusions that fit the experimental data with χ = 3.5, 2.8 or 2.4 for P_6, P_3 and P_1 symmetry, respectively. The fit and corresponding envelope for P_6 are shown in Figures 5 and 6B. As the resolution of the *ab initio* modelling was insufficient to determine the locations of the PEG chains, constrained rigid body modelling was performed in CORAL.[54] Chains of 22 dummy residues, based on Svergun's approximation,[60] were used to model the Fuc-PEG. The Fuc-PEG appendages were constrained to the known fucose-binding sites (at residues Trp31 and Trp76 of the inter- and intra-monomeric binding sites).[32,35] The resulting model gave good fits to the scattering data (χ = 2.4) and overlaid neatly with the P_6 *ab initio* envelope (Figure 6B). Irrespective of the modelling strategy and in agreement with earlier studies[11,60,69] the Fuc-PEG chains were observed to extend away from the protein core, rather than interact with the protein surface. Therefore, the SAXS data were consistent with the proposed "Medusa complex".

RSL and Fuc-PEG are an interesting model system in the context of the "grafting distance" (D_G) and the Flory dimension (R_F) of the polymer.[11,60] The fucose-binding sites in RSL have a hexagonal arrangement with an edge length of ~2 nm (distance between the methyl substituents in Me-fuc crystal structure, PDB 2bt9). PEG 2000 has a R_F of ~3.5 nm, which is ~1.7-fold the grafting distance (nearest neighbours). As $D_G < R_F$ the tendency is for the PEG to adopt an extended "brush" conformation and thereby reduce steric interactions between the polymer chains. This model is well-represented by the SAXS data (Figure 6B).

Conclusions

We have demonstrated the possibility of noncovalent PEGylation in a protein-polymer conjugate based on the hexavalent lectin RSL and a fucose-capped PEG. A variety of biophysical techniques were used to characterize complex formation. By using NMR spectroscopy it was confirmed that the glycopolymer interacts with the fucose-binding sites of the protein. The chemical shift perturbation plot was consistent with previously obtained data for the binding of "fucose like" sugars.[35] The increase in NMR line widths and the necessity of the TROSY pulse sequence were indicative of an increased molecular weight (slower tumbling time) of the conjugate. The K_d for Fuc-PEG binding was estimated at ~1.3 μM by ITC measurements and the

reversible nature of the complex was demonstrated by competition experiments. The Fuc-PEG appendages were displaced by the tighter binding Me-fuc (while the weaker binding L-gal had no effect). Small angle X-ray scattering was used to elucidate the structure of the conjugate. The scattering data were consistent with a protein-polymer "Medusa complex" in which the PEG chains were extended from the protein core. In terms of broader applications, noncovalent PEGylation could involve proteins with an engineered sugar-binding site and a glyco-PEG with appropriate sugar functionality and PEG size. Alternatively, glyco-PEGs could be used as modifiers in drug delivery systems where lectin-bioadhesives control recognition and targeting.[37-39]

Supporting Information

Synthetic scheme and spectral characterisation of intermediates and Fuc-PEG; SEC of RSL bound to Fuc-PEG or Me-fuc; HSQC and TROSY-HSQC of RSL in ligand-free and -bound forms; Line-width analysis of RSL resonances; TROSY-HSQC of PEG 2000 control experiment; ITC data for RSL binding to Fuc-PEG.

Acknowledgements This research was supported by Teagasc (Walsh fellowship to PMA), NUI Galway (NMR infrastructure support and Millennium Fund to PBC), the Leverhulme Trust (grant F/00128/BO to AME), the EU COST Action (TD1003 Bioinspired Nanotechnologies) and Science Foundation Ireland (grants 10/RFP/BIC2807 and 13/CDA/2168 to PBC). We thank M. L. Rennie (NUI Galway) for assistance with ITC data analysis, R. Doohan (NUI Galway) for maintaining the NMR facility, and M. Wimmerová (Masaryk University) for providing the pET25rsl plasmid. The ESRF is gratefully acknowledged for the provision of beam time and experimental support.

References

(1) Kochendoerfer, G. G.; Chen, S.-Y.; Mao, F.; Cressman, S.; Traviglia, S.; Shao, H.; Hunter, C. L.; Low, D. W.; Cagle, E. N.; Carnevali, M.; Gueriguian, V.; Keogh, P. J.; Porter, H.; Stratton, S. M.; Wiedeke, M. C.; Wilken, J.; Tang, J.; Levy, J. J.; Miranda, L. P.; Crnogorac, M. M.; Kalbag, S.; Botti, P.; Schindler-Horvat, J.; Savatski, L.; Adamson, J. W.; Kung, A.; Kent, S. B. H.; Bradburne, J. A. *Science* **2003**, *299*, 884–887.

(2) Tao, L.; Mantovani, G.; Lecolley, F.; Haddleton, D. M. *J. Am. Chem. Soc.* **2004**, *126*, 13220–13221.

(3) Canalle, L. A.; Lowik, D. W. P. M.; van Hest, J. C. M. *Chem. Soc. Rev.* **2010**, *39*, 329–353.

(4) Keefe, A. J.; Jiang, S. *Nat. Chem.* **2012**, *4*, 59–63.

(5) Mancini, R. J.; Lee, J.; Maynard, H. D. *J. Am. Chem. Soc.* **2012**, *134*, 8474–8479.

(6) Nguyen, T. H.; Kim, S.-H.; Decker, C. G.; Wong, D. Y.; Loo, J. A.; Maynard, H. D. *Nat. Chem.* **2013**, *5*, 221–227.

(7) van Eldijk, M. B.; Smits, F. C. M.; Vermue, N.; Debets, M. F.; Schoffelen, S.; van Hest, J. C. M. *Biomacromolecules* **2014**, *15*, 2751–2759.

(8) Broyer, R. M.; Grover, G. N.; Maynard, H. D. *Chem. Commun.* **2011**, *47*, 2212–2226.

(9) Caliceti, P.; Veronese, F. M. *Adv. Drug Deliv. Rev.* **2003**, *55*, 1261–1277.

(10) Kontos, S.; Hubbell, J. A. *Chem. Soc. Rev.* **2012**, *41*, 2686–2695.

(11) Cattani, G.; Vogeley, L.; Crowley, P. B. *Nat. Chem.* **2015**, *7*, 823–828.

(12) Peleg-Shulman, T.; Tsubery, H.; Mironchik, M.; Fridkin, M.; Schreiber, G.; Shechter, Y. *J. Med. Chem.* **2004**, *47* , 4897–4904.

(13) Pasut, G.; Mero, A.; Caboi, F.; Scaramuzza, S.; Sollai, L.; Veronese, F. M. *Bioconjug. Chem.* **2008**, *19*, 2427–2431.

(14) Serwa, R.; Majkut, P.; Horstmann, B.; Swiecicki, J.-M.; Gerrits, M.; Krause, E.; Hackenberger, C. P. R. *Chem. Sci.* **2010**, *1*, 596–602.

(15) Chen, J.; Zhao, M.; Feng, F.; Sizovs, A.; Wang, J. *J. Am. Chem. Soc.* **2013**, *135*, 10938–10941.

(16) Boerakker, M. J.; Hannink, J. M.; Bomans, P. H. H.; Frederik, P. M.; Nolte, R. J. M.; Meijer, E. M.; Sommerdijk, N. A. J. M. *Angew. Chemie Int. Ed.* **2002**, *41*, 4239–4241.

(17) Sandanaraj, B. S.; Vutukuri, D. R.; Simard, J. M.; Klaikherd, A.; Hong, R.; Rotello, V. M.; Thayumanavan, S. *J. Am. Chem. Soc.* **2005**, *127*, 10693–10698.

(18) Wurm, F.; Klos, J.; Rader, H. J.; Frey, H. *J. Am. Chem. Soc.* **2009**, *131*, 7954–7955

(19) Biedermann, F.; Rauwald, U.; Zayed, J. M.; Scherman, O. A. *Chem. Sci.* **2011**, *2*, 279–286.

(20) Khondee, S.; Olsen, C. M.; Zeng, Y.; Middaugh, C. R.; Berkland, C. *Biomacromolecules* **2011**, *12*, 3880–3894.

(21) Mero, A.; Ishino, T.; Chaiken, I.; Veronese, F. M.; Pasut, G. *Pharm. Res.* **2011**, *28*, 2412–2421.

(22) Kurinomaru, T.; Tomita, S.; Kudo, S.; Ganguli, S.; Nagasaki, Y.; Shiraki, K. *Langmuir* **2012**, *28*, 4334–4338.

(23) Mueller, C.; Capelle, M. A. H.; Seyrek, E.; Martel, S.; Carrupt, P.-A.; Arvinte, T.; Borchard, G. *J. Pharm. Sci.* **2012**, *101*, 1995–2008.

(24) Kim, T. H.; Swierczewska, M.; Oh, Y.; Kim, A.; Jo, D. G.; Park, J. H.; Byun, Y.; Sadegh-Nasseri, S.; Pomper, M. G.; Lee, K. C.; Lee, S. *Angew. Chemie Int. Ed.* **2013**, *52* , 6880–6884.

(25) Wei, K.; Li, J.; Chen, G.; Jiang, M. *ACS Macro Lett.* **2013**, *2*, 278–283.

(26) Ambrosio, E.; Barattin, M.; Bersani, S.; Shubber, S.; Uddin, S.; van der Walle, C. F.; Caliceti, P.; Salmaso, S. *J. Control. Release* **2016**, *226*, 35–46.

(27) Sakai, F.; Yang, G.; Weiss, M. S.; Liu, Y.; Chen, G.; Jiang, M. *Nat Commun* **2014**, *5*, 4634.

(28) Ng, S.; Lin, E.; Kitov, P. I.; Tjhung, K. F.; Gerlits, O. O.; Deng, L.; Kasper, B.; Sood, A.; Paschal, B. M.; Zhang, P.; Ling, C.-C.; Klassen, J. S.; Noren, C. J.; Mahal, L. K.; Woods, R. J.; Coates, L.; Derda, R. *J. Am. Chem. Soc.* **2015**, *137* , 5248–5251.

(29) Kula, M.-R.; Johansson, G.; Bückmann, A. F. *Biochem. Soc. Trans.* **1979**, *7* , 1–5. Coincidentally, this data was presented at a Biochemical Society meeting in Galway.

(30) Johansson, G.; Joelsson, M. *Anal. Biochem.* **1986**, *158*, 104–110.

(31) Kopperschläger, G.; Kirchberger, J. In *Aqueous Two-Phase Systems: Methods and Protocols*; Hatti-Kaul, R., Ed.; Humana Press: Totowa, New Jersey, 2000; pp 329–344.

(32) Kostlanova, N.; Mitchell, E. P.; Lortat-Jacob, H.; Oscarson, S.; Lahmann, M.; Gilboa-Garber, N.; Chambat, G.; Wimmerova, M.; Imberty, A. *J. Biol. Chem.* **2005**, *280*, 27839–

27849.

(33) Arnaud, J.; Claudinon, J.; Tröndle, K.; Trovaslet, M.; Larson, G.; Thomas, A.; Varrot, A.; Römer, W.; Imberty, A.; Audfray, A. *ACS Chem. Biol.* **2013**, *8*, 1918–1924.

(34) Arnaud, J.; Tröndle, K.; Claudinon, J.; Audfray, A.; Varrot, A.; Römer, W.; Imberty, A. *Angew. Chemie Int. Ed.* **2014**, *53*, 9267–9270.

(35) Antonik, P. M.; Volkov, A. N.; Broder, U. N.; Lo Re, D.; Van Nuland, N. A. J.; Crowley, P. B. *Biochemistry* **2016**, *55*, 1195−1203.

(36) Ravera, E.; Ciambellotti, S.; Cerofolini, L.; Martelli, T.; Kozyreva, T.; Bernacchioni, C.; Giuntini, S.; Fragai, M.; Turano, P.; Luchinat, C. *Angew. Chemie Int. Ed.* **2016**, *55*, 2446–2449.

(37) Lu, Z.-R.; Gao, S.-Q.; Kopečková, P.; Kopeček, J. *Bioconjug. Chem.* **2000**, *11*, 3–7.

(38) Bies, C.; Lehr, C.-M.; Woodley, J. F. *Adv. Drug Deliv. Rev.* **2004**, *56*, 425–435.

(39) Neutsch, L.; Wirth, E.-M.; Spijker, S.; Pichl, C.; Kählig, H.; Gabor, F.; Wirth, M. *J. Control. Release* **2013**, *169*, 62–72.

(40) Kolb, H. C.; Finn, M. G.; Sharpless, K. B. *Angew. Chemie Int. Ed.* **2001**, *40*, 2004–2021.

(41) Eissa, A. M.; Khosravi, E.; Cimecioglu, A. L. *Carbohydr. Polym.* **2012**, *90*, 859–869.

(42) Ni, J.; Singh, S.; Wang, L.-X. *Bioconjug. Chem.* **2003**, *14*, 232–238.

(43) Pervushin, K.; Riek, R.; Wider, G.; Wüthrich, K. *Proc. Natl. Acad. Sci.* **1997**, *94*, 12366–12371.

(44) Weigelt, J. *J. Am. Chem. Soc.* **1998**, *120*, 12706.

(45) Delaglio, F.; Grzesiek, S.; Vuister, G. W.; Zhu, G.; Pfeifer, J.; Bax, A. *J. Biomol. NMR* **1995**, *6*, 277–293.

(46) Vranken, W. F.; Boucher, W.; Stevens, T. J.; Fogh, R. H.; Pajon, A.; Llinas, P.; Ulrich, E. L.; Markley, J. L.; Ionides, J.; Laue, E. D. *Proteins* **2005**, *59* , 687–696.

(47) Williamson, M. P. *Prog. Nucl. Magn. Reson. Spectrosc.* **2013**, *73*, 1–16.

(48) Pernot, P.; Theveneau, P.; Giraud, T.; Fernandes, N. R.; Nurizzo, D.; Spruce, D.; Surr, J.; McSweeney, S.; Round, A.; Felisaz, F.; Foedinger, L.; Gobbo, A.; Huet, J.; Villard, C.; Cipriani, F. *J. Phys. Conf. Ser.* **2010**, *247*, 12009.

(49) Pernot, P.; Round, A.; Barrett, R.; De Maria Antolinos, A.; Gobbo, A.; Gordon, E.; Huet, J.; Kieffer, J.; Lentini, M.; Mattenet, M.; Morawe, C.; Mueller-Dieckmann, C.; Ohlsson, S.; Schmid, W.; Surr, J.; Theveneau, P.; Zerrad, L.; McSweeney, S. *J. Synchrotron Radiat.*

2013, *20*, 660–664.

(50) Round, A.; Felisaz, F.; Fodinger, L.; Gobbo, A.; Huet, J.; Villard, C.; Blanchet, C. E.; Pernot, P.; McSweeney, S.; Roessle, M.; Svergun, D. I.; Cipriani, F. *Acta Crystallogr. Sect. D Biol. Crystallogr.* **2015**, *71*, 67–75.

(51) Round, A.; Brown, E.; Marcellin, R.; Kapp, U.; Westfall, C. S.; Jez, J. M.; Zubieta, C. *Acta Crystallogr. Sect. D* **2013**, *69*, 2072–2080.

(52) Brennich, M. E.; Kieffer, J.; Bonamis, G.; De Maria Antolinos, A.; Hutin, S.; Pernot, P.; Round, A. *J. Appl. Crystallogr.* **2016**, *49*, 203–212.

(53) Petoukhov, M. V; Konarev, P. V; Kikhney, A. G.; Svergun, D. I. *J. Appl. Crystallogr.* **2007**, *40*, s223–s228.

(54) Petoukhov, M. V; Franke, D.; Shkumatov, A. V; Tria, G.; Kikhney, A. G.; Gajda, M.; Gorba, C.; Mertens, H. D. T.; Konarev, P. V; Svergun, D. I. *J. Appl. Crystallogr.* **2012**, *45*, 342–350.

(55) Konarev, P. V; Petoukhov, M. V; Volkov, V. V; Svergun, D. I. *J. Appl. Crystallogr.* **2006**, *39*, 277–286.

(56) Guinier, A. *Ann. Phys. (Paris).* **1939**, *12*, 161–237.

(57) Porod, G. In *Small angle X-ray scattering*; Glatter, O., Kratky, O., Eds.; Academic Press: London (UK), 1982; pp 17–51.

(58) Svergun, D. I. *J. Appl. Crystallogr.* **1992**, *25*, 495–503.

(59) Konarev, P. V; Volkov, V. V; Sokolova, A. V; Koch, M. H. J.; Svergun, D. I. *J. Appl. Crystallogr.* **2003**, *36*, 1277–1282.

(60) Svergun, D. I.; Ekstrom, F.; Vandegriff, K. D.; Malavalli, A.; Baker, D. A.; Nilsson, C.; Winslow, R. M. *Biophys. J.* **2008**, *94*, 173–181.

(61) Franke, D.; Svergun, D. I. *J. Appl. Crystallogr.* **2009**, *42*, 342–346.

(62) Volkov, V. V; Svergun, D. I. *J. Appl. Crystallogr.* **2003**, *36*, 860–864.

(63) Svergun, D.; Barberato, C.; Koch, M. H. J. *J. Appl. Crystallogr.* **1995**, *28*, 768–773.

(64) Kozin, M. B.; Svergun, D. I. *J. Appl. Crystallogr.* **2001**, *34*, 33–41.

(65) Fee, C. J.; Van Alstine, J. M. *Bioconjug. Chem.* **2004**, *15*, 1304–1313.

(66) Fee, C. J.; Van Alstine, J. M. In *Protein Purification*; John Wiley & Sons, Inc., 2011; pp 339–362.

(67) Crowley, P. B.; Chow, E.; Papkovskaia, T. *ChemBioChem* **2011**, *12*, 1043–1048.

(68) Crowley, P. B.; Brett, K.; Muldoon, J. *ChemBioChem* **2008**, *9*, 685–688.

(69) Pai, S. S.; Hammouda, B.; Hong, K. L.; Pozzo, D. C.; Przybycien, T. M.; Tilton, R. D. *Bioconjug. Chem.* **2011**, *22*, 2317–2323.

Figures

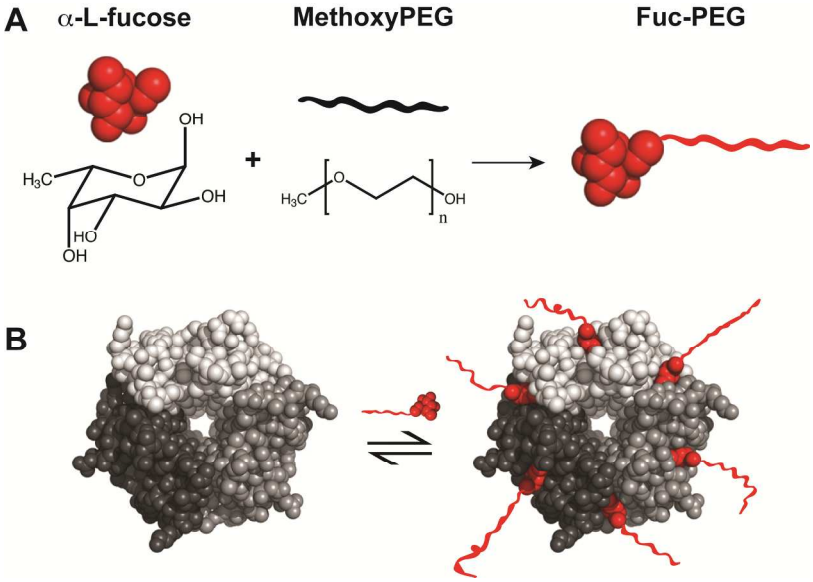

Figure 1. Simplified representations of **(A)** fucose-capped PEG (Fuc-PEG, see Scheme S1 for details) and **(B)** noncovalent PEGylation of RSL with Fuc-PEG (~2.3 kDa) to yield a protein-polymer "Medusa complex". Note that RSL is a hexavalent trimer with three intra-monomeric and three inter-monomeric sugar binding sites.[32,35]

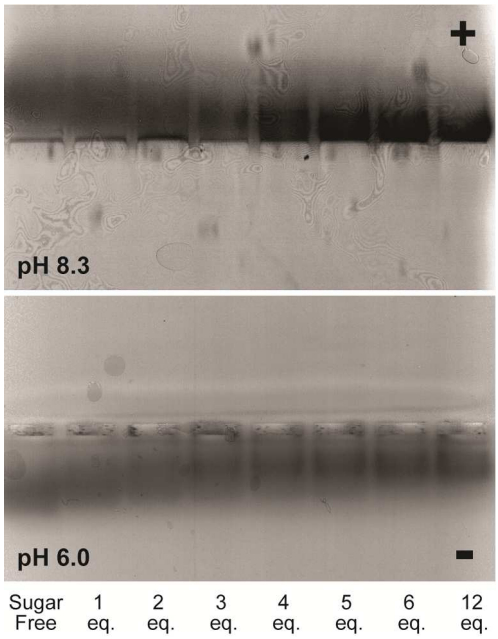

Figure 2. Native gel electrophoresis, 5 % polyacrylamide (top) or 2 % agarose (bottom panel), of RSL in the sugar-free or polymer bound form. The equivalents of Fuc-PEG, the buffer pH and the electrode locations are indicated.

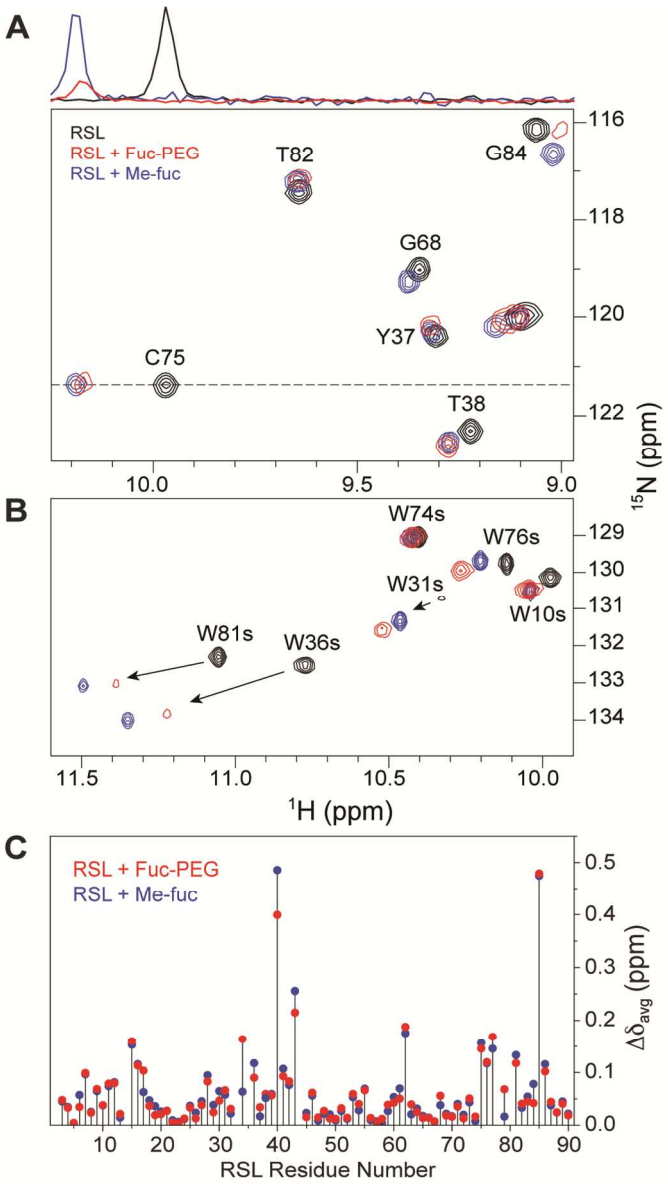

Figure 3. Spectral regions **(A)** and **(B)** from the overlaid ^{1}H-^{15}N TROSY-HSQC spectra of sugar-free RSL (black contours) and RSL bound to Fuc-PEG (red) or Me-fuc (blue). **(C)** Plot of the average chemical shift perturbations ($\Delta\delta_{avg}$) due to interaction of RSL with 12 eq. of Fuc-PEG (red) or Me-fuc (blue). The Me-fuc data were reported previously.[35]

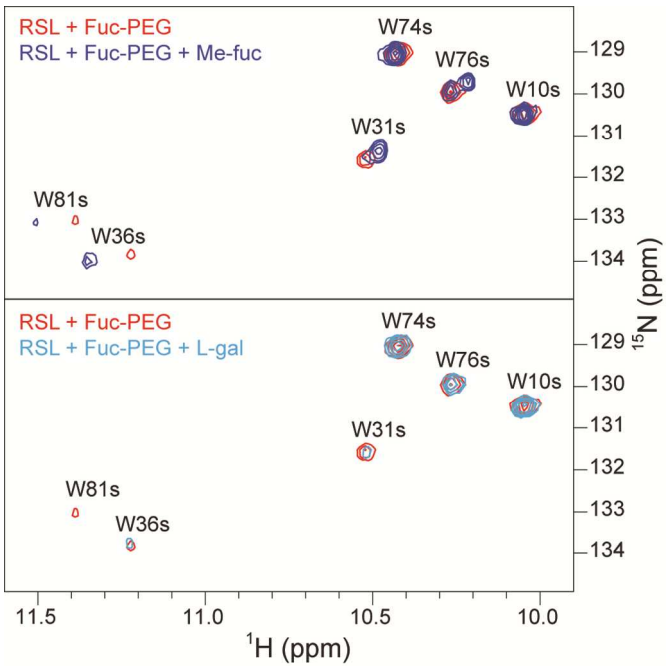

Figure 4. Spectral region from the overlaid TROSY-HSQC spectra of RSL in the presence of 6 equivalents of Fuc-PEG (red) and after the addition of 6 equivalents of Me-fuc (top) or L-gal (bottom panel).

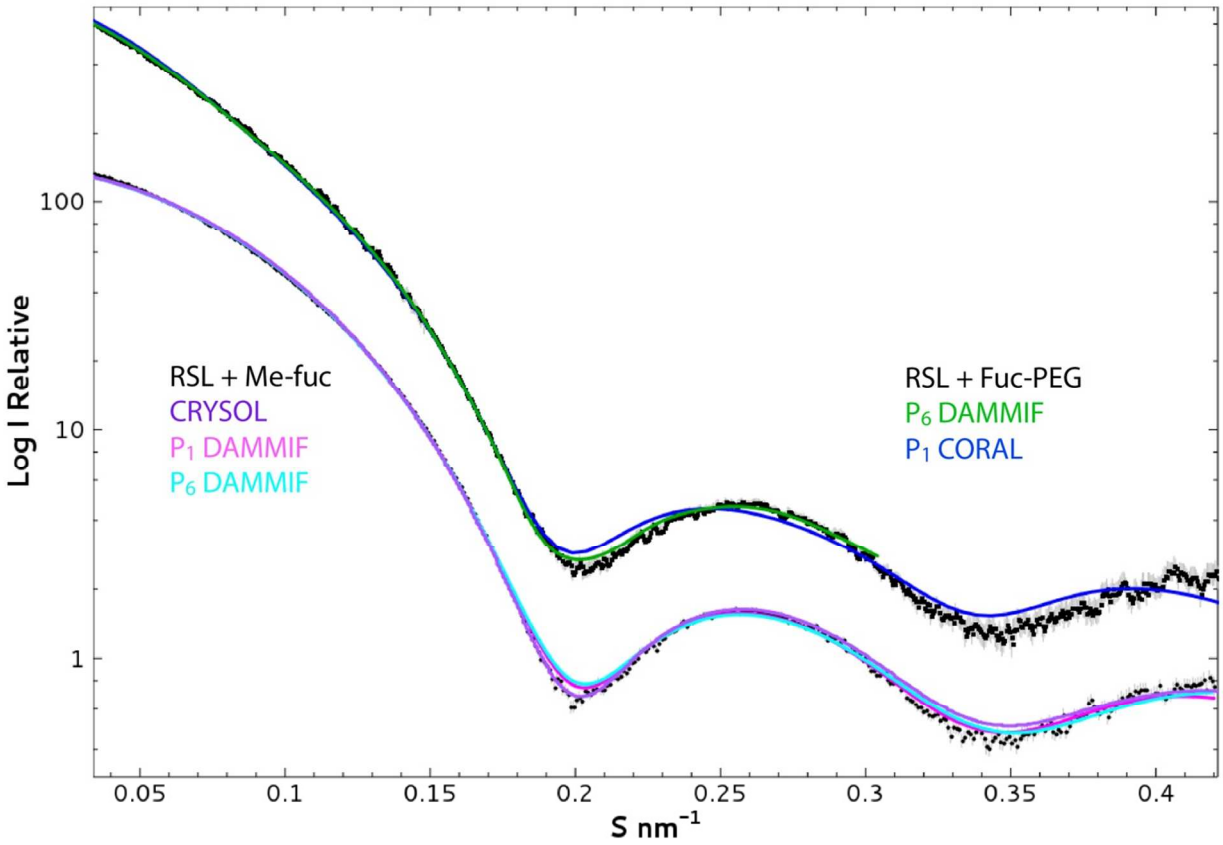

Figure 5. SAXS data and model fits for RSL bound to Me-fuc (lower curves) and RSL bound to Fuc-PEG (upper curves).

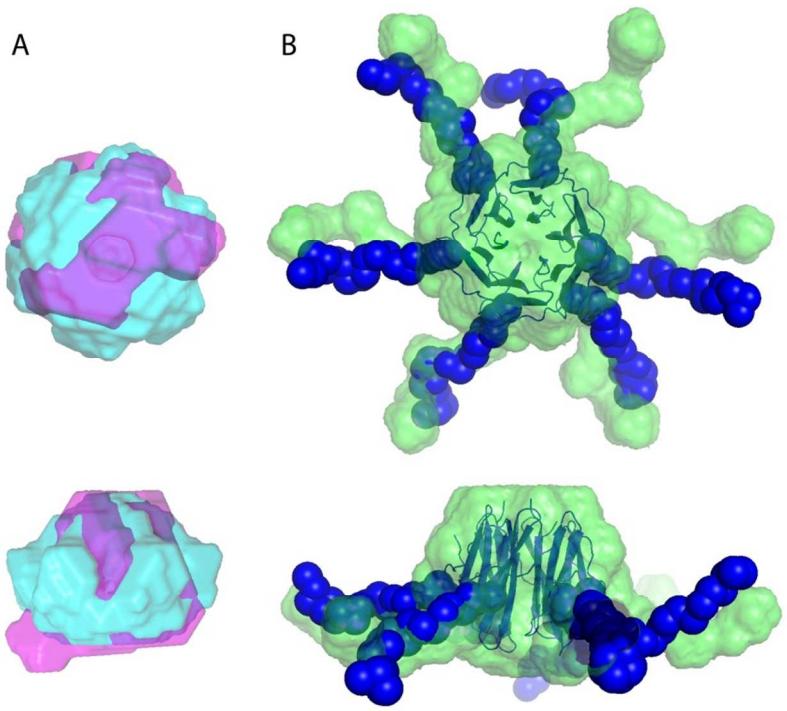

Figure 6. Top down and side views of the SAXS models of **(A)** RSL bound to Me-fuc and **(B)** RSL bound to Fuc-PEG. The models are colour-coded to match the fits in Figure 5. The DAMMIF models of RSL generated with P_1 or P_6 symmetry are coloured magenta and cyan, respectively. The DAMMIF (P_6) or CORAL (PEG chains only) models of RSL bound to Fuc-PEG are coloured green and blue, respectively.

TOC Graphic